

Sniffers, buzzers, toggles and blinkers: dynamics of regulatory and signaling pathways in the cell

John J Tyson^{*†}, Katherine C Chen^{*‡} and Bela Novak[§]

The physiological responses of cells to external and internal stimuli are governed by genes and proteins interacting in complex networks whose dynamical properties are impossible to understand by intuitive reasoning alone. Recent advances by theoretical biologists have demonstrated that molecular regulatory networks can be accurately modeled in mathematical terms. These models shed light on the design principles of biological control systems and make predictions that have been verified experimentally.

Addresses

^{*}Department of Biology, Virginia Polytechnic Institute and State University, Blacksburg, VA 24061, USA

[†]e-mail: tyson@vt.edu

[‡]e-mail: kchen@vt.edu

[§]Molecular Network Dynamics Research Group of Hungarian Academy of Sciences and Department of Agricultural Chemical Technology, Budapest University of Technology and Economics, 1521 Budapest, Gellert ter 4, Hungary

e-mail: bnovak@mail.bme.hu

Current Opinion in Cell Biology 2003, **15**:XXX–XXX

This review comes from a themed issue on
Cell regulation
Edited by Pier Paolo di Fiore and Pier Giuseppe Pelicci

0955-0674/03/\$ – see front matter
© 2003 Elsevier Science Ltd. All rights reserved.

Abbreviations

Cdk	cyclin-dependent kinase
CKI	cyclin-dependent kinase inhibitor
IP₃	inositol trisphosphate
MAPK	mitogen-activated protein kinase
MPF	M-phase-promoting factor (Cdk1–cyclin B)

Introduction

Since the advent of recombinant DNA technology about 20 years ago, molecular biologists have been remarkably successful in dissecting the molecular mechanisms that underlie the adaptive behavior of living cells. Stunning examples include the lysis–lysogeny switch of viruses [1], chemotaxis in bacteria [2], the DNA-division cycle of yeasts [3], segmentation patterns in fruit fly development [4] and signal transduction pathways in mammalian cells [5]. When the information in any of these cases is laid out in graphical form

(http://discover.nci.nih.gov/kohnk/interaction_maps.html; http://www.csa.ru:82/Inst/gorb_dep/inbios/genet/s0ntwk.htm; <http://www.biocarta.com/genes/index.asp>), the molecular network looks strikingly similar to the wiring diagram of a modern electronic gadget. Instead of resistors, capacitors and transistors hooked together by wires, one sees genes, proteins and metabolites hooked together by chemical reactions and intermolecular interactions. The temptation is irresistible to ask whether physiological regulatory systems can be understood in mathematical

terms, in the same way an electrical engineer would model a radio [6]. Preliminary attempts at this sort of modeling have been carried out in each of the cases mentioned above [7–11,12^{**},13,14,15^{**}].

To understand how these models are built and why they work the way they do, one must develop a precise mathematical description of molecular circuitry and some intuition about the dynamical properties of regulatory networks. Complex molecular networks, like electrical circuits, seem to be constructed from simpler modules: sets of interacting genes and proteins that carry out specific tasks and can be hooked together by standard linkages [16]. Excellent reviews from other perspectives can be found elsewhere [17,18^{*},19–22,23^{*},24^{*},25], and also book-length treatments [26–29].

In this review, we show how simple signaling pathways can be embedded in networks using positive and negative feedback to generate more complex behaviors—toggle switches and oscillators—which are the basic building blocks of the exotic, dynamic behavior shown by nonlinear control systems. Our purpose is to present a precise vocabulary for describing these phenomena and some memorable examples of each. We hope that this review will improve the reader's intuition about molecular dynamics, foster more accurate discussions of the issues, and promote closer collaboration between experimental and computational biologists.

Linear and hyperbolic signal-response curves

Let's start with two simple examples of protein dynamics: synthesis and degradation (Figure 1a), and phosphorylation and dephosphorylation (Figure 1b). Using the law of mass action, we can write rate equations for these two mechanisms, as follows:

$$(a) \frac{dR}{dt} = k_0 + k_1 S - k_2 R,$$

$$(b) \frac{dR_P}{dt} = k_1 S (R_T - R_P) - k_2 R_P.$$

In case (a), S = signal strength (e.g. concentration of mRNA) and R = response magnitude (e.g. concentration of protein). In case (b), R_P is the phosphorylated form of the response element (which we suppose to be the active form), $R_P = [RP]$, and

$R_T = R + R_P$ = total concentration of the response element.

A steady-state solution of a differential equation, $dR/dt = f(R)$, is a constant, R_{ss} , that satisfies the algebraic equation $f(R_{ss}) = 0$. In our cases,

$$(a) R_{ss} = \frac{k_0 + k_1 S}{k_2}$$

$$(b) R_{P,ss} = \frac{R_T S}{(k_2/k_1) + S}.$$

These equations correspond to the linear and hyperbolic signal-response curves in Figure 1. In most cases, these

simple components are embedded in more complex pathways, to generate signal-response curves of more adaptive value.

Sigmoidal signal-response curves

Case (c) of Figure 1 is a modification of case (b), where the phosphorylation and dephosphorylation reactions are governed by Michaelis-Menten kinetics:

$$(c) \quad \frac{dR_p}{dt} = \frac{k_1 S(R_T - R_p)}{K_{m1} + R_T - R_p} - \frac{k_2 R_p}{K_{m2} + R_p}.$$

In this case, the steady-state concentration of the phosphorylated form is a solution of the quadratic equation:

$$k_1 S(R_T - R_p)(K_{m2} + R_p) = k_2 R_p(K_{m1} + R_T - R_p).$$

The biophysically acceptable solution ($0 < R_p < R_T$) of this equation is [30]:

$$(c) \quad \frac{R_{p,ss}}{R_T} = G(k_1 S, k_2, \frac{K_{m1}}{R_T}, \frac{K_{m2}}{R_T}),$$

where the ‘Goldbeter-Koshland’ function, G , is defined as:

$$G(u, v, J, K) =$$

$$\frac{2uK}{v - u + vJ + uK + \sqrt{(v - u + vJ + uK)^2 - 4(v - u)uK}}.$$

In Figure 1c, column 3, we plot $R_{p,ss}$ as a function of S : it is a sigmoidal curve if J and K are both $\ll 1$. This mechanism for creating a switch-like signal-response curve is called zero-order ultrasensitivity.

The Goldbeter–Koshland function, although switch-like, shares with linear and hyperbolic curves the properties of being graded and reversible. By ‘graded’ we mean that the response increases continuously with signal strength. A slightly stronger signal gives a slightly stronger response. The relationship is ‘reversible’ in the sense that if signal strength is changed from S_{initial} to S_{final} , the response at S_{final} is the same whether the signal is being increased ($S_{\text{initial}} < S_{\text{final}}$) or decreased ($S_{\text{initial}} > S_{\text{final}}$). Although continuous and reversible, a sigmoidal response is abrupt. Like a buzzer or a laser pointer, to activate the response one must push hard enough on the button, and to sustain the response one must keep pushing. When one lets up on the button, the response switches off at precisely the same signal strength at which it switched on.

Perfectly adapted signal-response curves

By supplementing the simple linear response element (Figure 1a) with a second signaling pathway (through species X in Figure 1d), we can create a response mechanism that exhibits perfect adaptation to the signal. Perfect adaptation means that although the signaling pathway exhibits a transient response to changes in signal strength, its steady-state response R_{ss} is independent of S . Such behavior is typical of chemotactic systems, which respond to an abrupt change in attractants or repellants, but then adapt to a constant level of the signal. Our own sense of smell operates this way, so we refer to this type of response as a ‘sniffer.’

The hyperbolic response element (Figure 1b) can also be made perfectly adapted by adding a second signaling pathway that down regulates the response. Levchenko and Iglesias [31*] have used a mechanism of this sort to model phosphoinositide signaling in slime mold cells and neutrophils.

Many authors have presented models of perfect adaptation (see [32–35] for representative published work).

Positive feedback: irreversible switches

In Figure 1d the signal influences the response via two parallel pathways that push the response in opposite directions (an example of feed-forward control). Alternatively, some component of a response pathway may feed back on the signal. Feedback can be positive, negative or mixed.

There are two types of positive feedback. In Figure 1e, R activates protein E (by phosphorylation), and EP enhances the synthesis of R . In Figure 1f, E promotes the degradation of R ; hence, R and E are mutually antagonistic. In either case (mutual activation or antagonism), positive feedback may create a discontinuous switch, meaning that the cellular response changes abruptly and irreversibly as signal magnitude crosses a critical value. For instance, in Figure 1e, as signal strength (S) increases, the response is low until S exceeds some critical intensity, S_{crit} , at which point the response increases abruptly to a high value. Then, if S decreases, the response stays high (i.e. the switch is irreversible; unlike a sigmoidal response, which is reversible). Notice that, for S values between 0 and S_{crit} , the control system is ‘bistable’ — that is, it has two stable steady-state response values (on the upper and lower branches — the solid lines) separated by an unstable steady state (on the intermediate branch — the dashed line).

The signal-response curves in Figure 1e,f would be called ‘one-parameter bifurcation diagrams’ by an applied mathematician. The parameter is signal strength (manipulable by the experimenter). The steady-state response, on the Y axis, is an indicator of the behavior of the control system as a function of the signal. At S_{crit} , the behavior of the control system changes abruptly and irreversibly from low response to high response (or *vice versa*). Such points of qualitative change in the behavior of a nonlinear control system are called bifurcation points; in this case, a ‘saddle-node bifurcation point’. We will shortly meet other, more esoteric bifurcation points, associated with more complex signal-response relationships.

Discontinuous responses come in two varieties: the one-way switch (e.g. Figure 1e), and the toggle switch (e.g. Figure 1f). One-way switches presumably play major roles in developmental processes characterized by a point-of-no-return (see, for example, [21]). Apoptosis is another decision that must be irreversible in this sense. A particularly clear experimental example is frog oocyte maturation in response to progesterone [36].

In the toggle switch, if S is decreased enough, the switch will go back to the off-state, as in Figure 1f (column 3). For intermediate stimulus strengths ($S_{\text{crit1}} < S < S_{\text{crit2}}$), the

response of the system can be either small or large, depending on how S was changed. This sort of two-way, discontinuous switch is often referred to as hysteresis. Nice examples include the *lac* operon in bacteria [21], the activation of M-phase-promoting factor (MPF) in frog egg extracts [37], and the autocatalytic conversion of normal prion protein to its pathogenic form [38**]. Bistable behavior of MPF in frog egg extracts has recently been confirmed experimentally by two groups: Sha *et al.* [39], and Pomerening and Ferrell (personal communication). Chen *et al.* [9] proposed that a toggle switch governs the ‘start’ and ‘finish’ transitions in the budding yeast cell cycle, and this prediction was confirmed recently in an elegant experiment by Cross *et al.* [40**].

Toggle switches have also been realized in artificial genetic networks based on mutual inhibition [41] or mutual activation [42*]. These networks were designed and built in explicit reliance on theoretical ideas of the kind we have described.

Negative feedback: homeostasis and oscillations

In negative feedback, the response counteracts the effect of the stimulus. In Figure 1g, the response element, R, inhibits the enzyme catalyzing its synthesis; hence, the rate of production of R is a sigmoidal decreasing function of R. The signal in this case is the demand for R (i.e. the rate of consumption of R is given by k_2SR). The steady state concentration of R is confined to a narrow window for a broad range of signal strengths, because the supply of R adjusts to its demand. This type of regulation, commonly employed in biosynthetic pathways, is called homeostasis. It is a kind of imperfect adaptation, but it is not a sniffer because stepwise increases in S do not generate transient changes in R.

Negative feedback can also create an oscillatory response. A two-component, negative feedback loop, $X \rightarrow R \rightarrow X$, can exhibit damped oscillations to a stable steady state but not sustained oscillations [43]. Sustained oscillations require at least three components: $X \rightarrow Y \rightarrow R \rightarrow X$. The third component (Y) introduces a time delay in the feedback loop, causing the control system repeatedly to overshoot and undershoot its steady state.

In Figure 2a (column 1), we present a wiring diagram for a negative-feedback control loop. For intermediate signal strengths, the steady-state response of the control system is unstable, and the system executes sustained oscillations (column 2) in the variables $X(t)$, $Y_p(t)$ and $R_p(t)$. In the signal-response curve (column 3), we plot $R_{p,ss}$ as a function of S , noting that the steady-state response is unstable for $S_{crit1} < S < S_{crit2}$. Within this range, $R_p(t)$ oscillates between $R_{p,min}$ and $R_{p,max}$ (the lower and upper filled circles, respectively). In the terminology introduced earlier, S_{crit1} and S_{crit2} are bifurcation points, where the steady-state response changes its stability and oscillations arise by a generic mechanism called a ‘Hopf bifurcation.’ As S moves away from either bifurcation point, the amplitude of oscillation increases.

Negative feedback has been proposed as a basis for oscillations in protein synthesis [44], MPF activity [45], MAPK signaling pathways [46], and circadian rhythms [47,48,49*].

Using similar theoretical ideas about negative feedback oscillators, Elowitz and Leibler [50] designed an artificial genetic network consisting of three operons that repressed one another in a loop. In order to satisfy the theoretical expectations for sustained oscillations, these authors engineered the three proteins to be unstable, with roughly equal half-lives. Individual bacteria containing these plasmids showed periodic expression of a fluorescent reporter protein, qualifying this case as a literal ‘blinker’.

Positive and negative feedback: oscillators

Oscillations often arise in systems containing both positive feedback (autocatalysis) and negative feedback (Figure 2b,c). The positive-feedback loop creates a bistable system (a toggle switch) and the negative-feedback loop drives the system back and forth between the two stable steady states. Oscillators of this sort come in two varieties.

Activator-inhibitor oscillators

In Figure 2b, R is created in an autocatalytic process, and then it promotes the production of an inhibitor, X, which either slows down R production or speeds up R removal. First, R builds up, then comes X to force R back down, then X disappears and R can rise again.

In the second column of Figure 2b, we plot a ‘phase portrait’ of the activator-inhibitor oscillator, illustrating the notion that the negative-feedback loop drives the bistable system back and forth between its two steady-state regimes. First, consider X to be the signal and R to be the response, and plot (red curve) R_{ss} as a function of X. We get an S-shaped signal-response curve, indicating that the network functions as a toggle switch. For intermediate values of X, the control system is bistable (R_{ss} can be either small or large). Conversely, plotting X_{ss} (response) as a function of R (signal), we get a simple linear response curve (blue). Mathematicians refer to these curves as the R-nullcline ($dR/dt = 0$, red) and the X-nullcline ($dX/dt = 0$, blue). Where the two curves intersect (o) is a steady state for the full system, but the control system does not settle on this steady state because it is unstable. Instead, the variables, $R(t)$ and $X(t)$, oscillate around the steady state on a closed orbit (black curve, called a stable limit cycle). Such behavior is called a hysteresis oscillator, and the closed orbit is called a hysteresis loop.

The classic example of an activator-inhibitor system is cyclic AMP production in the slime mold, *Dictyostelium discoideum* [51]. External cAMP binds to a surface receptor, which stimulates adenylate cyclase to produce and excrete more cAMP. At the same time, cAMP-binding pushes the receptor into an inactive form. After cAMP falls off, the inactive form slowly recovers its ability to bind cAMP and stimulate adenylate cyclase again. This mechanism lies behind all the curious properties of the cAMP signaling system in *Dictyostelium*: oscillations, relay, adaptation, and wave propagation. (For details, see [27].)

Substrate-depletion oscillators

In Figure 2c, X is converted into R in an autocatalytic process. Suppose, at first, X is abundant and R is scarce. As R builds up, the production of R accelerates until there is an explosive conversion of the entire pool of X into R. Then the autocatalytic reaction shuts off for lack of substrate, X. R is degraded, and X must build up again before another burst of R is produced.

This is essentially the mechanism of MPF oscillations in frog egg extracts [37,52]. MPF is a dimer of a kinase subunit, cyclin-dependent kinase 1 (Cdk1), and a regulatory subunit, cyclin B. As cyclin B accumulates in the extract, it combines rapidly with Cdk1 (in excess). The dimer is immediately inactivated by phosphorylation of the kinase subunit (X in Figure 2c is cyclin B–Cdk1-P). X can be converted into active MPF (R in Figure 2c is the unphosphorylated form of cyclin B–Cdk1) by a phosphatase called Cdc25 (EP in the figure). Active MPF activates Cdc25 by phosphorylating it. The true MPF story is considerably more complicated than just described, but in broad strokes it is a substrate-depletion oscillator.

The signal-response curve for this mechanism is plotted in column 3 of Figure 2c. The signal, S , is the rate of synthesis of substrate X. Low signal gives low response and high signal gives high response, as expected. But for S between S_{crit1} and S_{crit2} , the steady-state response is unstable and the response oscillates between R_{max} (upper filled circles) and R_{min} (lower filled circles). The oscillations are ‘born’ at Hopf bifurcations (at S_{crit1} and S_{crit2}), but there is a big difference between the Hopf bifurcations in Figure 2c and those in Figure 2a. In Figure 2a, the ‘newborn’ limit cycles (close to S_{crit}) are stable, whereas in Figure 2c they are unstable (as indicated by the open circles). As S departs from S_{crit} , the amplitude of the unstable limit cycle grows quickly, until the branch of unstable limit cycles connects smoothly with the branch of large amplitude, stable limit cycles (denoted by filled circles). To distinguish between these two possibilities, the bifurcations in Figure 2a are called ‘supercritical Hopfs’, and the ones in Figure 2c are called ‘subcritical’.

The distinction between super- and subcritical Hopf bifurcations has important physiological consequences. Look again at Figures 2a and c, and let us imagine that signal strength S is being reduced slowly from 8 to 4 in Figure 2a and from 0.4 to 0.2 in Figure 2c. In both cases, we pass a Hopf bifurcation at S_{crit2} . In case 2a, it is a supercritical Hopf bifurcation, and the oscillatory solutions appear, at first, with small amplitude, perhaps too small to generate a useful response. On the other hand, in case 2c, as S passes the subcritical Hopf bifurcation, stable oscillations of large amplitude appear abruptly. The control system immediately generates a large and robust response. When S is being changed in the opposite direction, the large amplitude periodic solutions disappear just as abruptly. Hence, subcritical Hopf bifurcations provide a general mechanism for hysteretic transitions between a stable steady state and a stable, large amplitude oscillation. In biophysical control systems, where membrane potential

oscillations can be measured with great accuracy, it is easy to distinguish the difference between sub- and supercritical Hopf bifurcations (e.g. [53]).

Complex networks: the cell cycle control system

The signal-response elements we have just described, buzzers, sniffers, toggles and blinkers, usually appear as components of more complex networks (see, for example, [7–11,12**]). Being most familiar with the regulatory network of the eukaryotic cell cycle, we use that example to illustrate the issues involved in modeling realistic wiring diagrams.

A generic wiring diagram for the Cdk network regulating DNA synthesis and mitosis is presented in Figure 3a. The network, involving proteins that regulate the activity of Cdk1–CycB heterodimers, consists of three modules that oversee the G1/S, G2/M and M/G1 transitions of the cell cycle. The G1/S module is a toggle switch, based on mutual inhibition between Cdk1–cyclin B and CKI, a stoichiometric cyclin-dependent kinase inhibitor. The G2/M module is a second toggle switch, based on mutual activation between Cdk1–cyclin B and Cdc25 (a phosphatase that activates the dimer), and mutual inhibition between CDK1–cyclin B and Wee1 (a kinase that activates the dimer). The M/G1 module is an oscillator, based on a negative-feedback loop: Cdk1–cyclin B activates the anaphase-promoting complex (APC), which activates Cdc20, which degrades cyclin B.

The ‘signal’ that drives cell proliferation is cell growth: a newborn cell cannot leave G1 and enter the DNA synthesis/division process (S/G2/M) until it grows to a critical size [54]. Hence, our signal-response curve is a plot of steady-state activity of Cdk1–cyclin B as a function of cell size (Figure 3b). The signal-response curve of the full network is complicated indeed, but it clearly has inherited the basic characteristics of its component modules. We can discern the typical S-shaped bistability curves of the G1/S and G2/M modules and the oscillatory solutions of the negative-feedback loop (the M/G1 module). The oscillatory solutions, generated by the negative-feedback loop, interact with the bistability curve of the G2/M module to create an ‘infinite-period’ bifurcation at cell size = 1.25. At this bifurcation (SN/IP), a stable steady state gives way to a large-amplitude periodic solution, and the period of oscillation is very long, for cell size close to 1.25. As size increases above 1.25, the period of oscillation drops dramatically.

In Figure 3b (red curve), progress through the cell cycle is viewed as a sequence of bifurcations. A small newborn cell (size = 0.73) is attracted to the stable G1 steady state (very low activity of Cdk1–cyclin B). As it grows, it eventually passes the saddle-node bifurcation (SN_s) where the G1 steady state disappears, and the cell makes an irreversible transition into S/G2 (moderate activity of Cdk1/cyclin B). It stays in S/G2 until it grows so large that the S/G2 steady state disappears, giving way to an infinite-period oscillation (SN/IP). CycB-dependent kinase activity soars, driving the cell into mitosis, and then plummets, as CycB is degraded by APC–Cdc20. The drop in Cdk1–cyclin B activity is the

signal for the cell to divide. Cell size drops from 1.46 to 0.73, and the control system is returned to its starting point, in the domain of attraction of the G1 steady state.

Signaling in space

So far, we have considered only time-dependent signaling. But spatial signaling also plays important roles in cell physiology (e.g. cell aggregation, somite formation, cell division plane localization, etc.). Interestingly the same mechanism (autocatalysis plus negative feedback) that creates oscillations (broken symmetry in time) can also create spatial patterns (broken symmetry in space) [55,56]. Two sorts of patterns may arise. If the inhibitor (or substrate) diffuses much more rapidly than the activator, activator piles up in local regions of space, forming steady-state (time-independent) patterns. On the other hand, when the diffusion constant of the inhibitor (or substrate) is about the same as (or less than) the diffusion constant of the activator, traveling waves of 'activation' propagate through the medium.

Steady-state patterns (commonly called 'Turing patterns') have been proposed for many time-independent, spatially periodic patterns in biology, such as animal coat patterns, leaf rudiment positioning, hair follicle distributions, and so on [57]. Traveling waves of cyclic AMP in fields of *Dictyostelium* amoebae govern the processes of aggregation, slug motility and fruiting [58,59].

Meinhardt and de Boer [60**] have recently presented an elegant model of division plane localization in *Escherichia coli*. In this model, FtsZ protein bound to the cell membrane promotes further FtsZ binding, at the expense of freely diffusible FtsZ in the cytoplasm. By Turing-type symmetry breaking, these interactions would create FtsZ rings at arbitrary positions along the bacterial axis. Interactions among Min proteins (C, D and E) create a pole-to-pole oscillating wave, which biases the FtsZ ring to form in the center of the cell.

Conclusions

The life of every organism depends crucially on networks of interacting proteins that detect signals and generate appropriate responses. Examples include chemotaxis, heat shock response, sporulation, hormone secretion, and cell-cycle checkpoints. Although diagrams and informal hand-waving arguments are often used to rationalize how these control systems work, such cartoons lack the precision necessary for a quantitative and reliable understanding of complex regulatory networks. To reprogram cellular control systems to our own specifications, we will need more exact, engineering-style representations of their wiring diagrams and governing equations.

Mathematical modeling and computer simulation of protein networks is a tool for formulating mechanistic hypotheses precisely and for deriving with confidence their physiological implications. In this review, we have shown how to create mathematical representations (nonlinear differential equations) of some simple signal-response elements, and how certain feedback and feed-forward signals can create diverse types of responses: sigmoidal

switches (buzzers), transient responses (sniffers), hysteretic switches (toggles), and oscillators (blinkers). From these components, nature has constructed regulatory networks of great complexity. With accurate mathematical representations of the individual components, we can assemble a computational model of any such network. By numerical simulation, we can compute the expected output of the network to any particular input.

A crucial point of contact between physiologists and applied mathematicians is the input-output relationship of a control system — what experimentalists call a signal-response curve, and theoreticians call a one-parameter bifurcation diagram. From the biologist's perspective, a signal-response curve summarizes the behavior of the biological control system. From the mathematician's perspective, a one-parameter bifurcation diagram summarizes the general, qualitative properties of solutions of a set of nonlinear differential equations. The theory of bifurcations assures us that there are only a few types of signal-response relationships, most of which have appeared in our examples. Irreversible transitions are associated with saddle-node bifurcations (Figure 1e). Oscillations arise at Hopf bifurcations (Figure 2a), and infinite-period bifurcations (Figure 3b). No matter how complicated the network or how rich its behavior, the signal-response curve can always be decomposed into these three bifurcations and a few others.

For the community of scientists to develop the sophisticated interplay of theory and experiment that will be needed to understand and manipulate molecular regulatory systems underlying cell physiology, we will first have to learn to communicate. Theoreticians must develop the vocabulary and intuition associated with genes, proteins and metabolites. And experimentalists must come to terms with differential equations, limit cycles and bifurcation diagrams. We hope this review will facilitate many new and fruitful dialogs.

Update

Recent work includes an elegant theoretical and experimental study of NF- κ B signaling [61**] and methods for deducing a molecular wiring diagram from a system's transient response to small disturbances [62*,63*].

Acknowledgements

We gratefully acknowledge financial support from the National Science Foundations of the USA (MCB-0078920) and Hungary (T 032015), from the Defense Advanced Research Project Agency (AFRL #F30602-02-0572), and from the James S McDonnell Foundation (21002050).

References and recommended reading

Papers of particular interest, published within the annual period of review, have been highlighted as:

- of special interest
 - of outstanding interest
1. Johnson AD, Poteete AR, Lauer G, Sauer RT, Ackers GK, Ptashne M: **Lambda repressor and cro — components of an efficient molecular switch.** *Nature* 1981, **294**:217-223.
 2. Falke JJ, Bass RB, Butler SL, Chervitz SA, Danielson MA: **The two-component signaling pathway of bacterial chemotaxis: a molecular view of signal transduction by receptors, kinases, and adaptation enzymes.** *Annu Rev Cell Dev Biol* 1997, **13**:457-512.

3. Mendenhall MD, Hodge AE: **Regulation of Cdc28 cyclin-dependent protein kinase activity during the cell cycle of the yeast *Saccharomyces cerevisiae***. *Microbiol Mol Biol Rev* 1998, **62**:1191-1243.
4. DiNardo S, Heemskerck J, Dougan S, O'Farrell PH: **The making of a maggot: patterning the *Drosophila* embryonic epidermis**. *Curr Opin Genet Dev* 1994, **4**:529-534.
5. Hanahan D, Weinberg RA: **The hallmarks of cancer**. *Cell* 2000, **100**:57-70.
6. Lazebnik Y: **Can a biologist fix a radio? Or, what I learned while studying apoptosis**. *Cancer Cell* 2002, **2**:179.
7. Arkin A, Ross J, McAdams H: **Stochastic kinetic analysis of developmental pathway bifurcation in phage λ -infected *Escherichia coli* cells**. *Genetics* 1998, **149**:1633-1648.
8. Bray D, Bourret RB, Simon MI: **Computer simulation of the phosphorylation cascade controlling bacterial chemotaxis**. *Mol Biol Cell* 1993, **4**:469-482.
9. Chen KC, Csikasz-Nagy A, Gyorffy B, Val J, Novak B, Tyson JJ: **Kinetic analysis of a molecular model of the budding yeast cell cycle**. *Mol Biol Cell* 2000, **11**:369-391.
10. von Dassow G, Meir E, Munro EM, Odell GM: **The segment polarity network is a robust developmental module**. *Nature* 2000, **406**:188-192.
11. Sharp DH, Reinitz J: **Prediction of mutant expression patterns using gene circuits**. *Biosystems* 1998, **47**:79-90.
- 12. Sanchez L, Thieffry D: **A logical analysis of the *Drosophila* gap-gene system**. *J Theor Biol* 2001, **211**:115-141.

As an alternative to modeling by differential equations, these authors describe pattern formation during a specific stage of fruit fly embryogenesis by a Boolean network, in which time, space and gene expression are represented by discrete (rather than continuous) variables.

13. Kholodenko BN, Demin OV, Moehren G, Hoek JB: **Quantification of short term signaling by the epidermal growth factor receptor**. *J Biol Chem* 1999, **274**:30169-30181.
14. Asthagiri AR, Lauffenburger DA: **Bioengineering models of cell signaling**. *Annu Rev Biomed Eng* 2000, **2**:31-53.
- 15. Shvartsman SY, Hagan MP, Yacoub A, Dent P, Wiley HS, Lauffenburger DA: **Autocrine loops with positive feedback enable context-dependent cell signaling**. *Am J Physiol* 2002, **282**:C545-C559.

These authors present a model of the mitogen-activated protein kinase (MAPK) signaling pathway, with both positive- and negative-feedback loops. The pathway's response to a transient signal can be either short-lived or persistent. Predictions of the model compared favorably to the activation of MAPK observed in human carcinoma cells exposed to short pulses of ionizing radiation.

16. Hartwell LH, Hopfield JJ, Leibler S, Murray AW: **From molecular to modular cell biology**. *Nature* 1999, **402**:C47-52.
17. Ferrell JE: **Self-perpetuating states in signal transduction: positive feedback, double-negative feedback and bistability**. *Curr Opin Cell Biol* 2002, **14**:140-148.
- 18. Ferrell J, Xiong W: **Bistability in cell signaling: how to make continuous processes discontinuous, and reversible processes irreversible**. *Chaos* 2001, **11**:227-236.

This is an easy-to-read introduction to bistable biological control systems based on graphical displays of the rate equations.

19. Hasty J, McMillen D, Isaacs F, Collins JJ: **Computational studies of gene regulatory networks: in numero molecular biology**. *Nat Rev Genet* 2001, **2**:268-279.
20. Tyson JJ, Chen K, Novak B: **Network dynamics and cell physiology**. *Nat Rev Mol Cell Biol* 2001, **2**:908-916.
21. Laurent M, Kellershohn N: **Multistability: a major means of differentiation and evolution in biological systems**. *Trends Biochem Sci* 1999, **24**:418-422.

22. Brazhnik P, de la Fuente A, Mendes P: **Gene networks: how to put the function in genomics**. *Trends Biotechnol* 2002, **20**:467-472.

- 23. Savageau M: **Design principles for elementary gene circuits: Elements, methods, and examples**. *Chaos* 2001, **11**:142-159.

See annotation Thomas and Kaufmann (2001) [24*].

- 24. Thomas R, Kauffman M: **Multistationarity, the basis of cell differentiation and memory. I. Structural conditions of multistationarity and other nontrivial behavior**. *Chaos* 2001, **11**:170-179.

These two reviews (see also Savageau [2001] [23*]) present modeling strategies that are considerably different from our approach (using differential equations based on detailed kinetic mechanisms). Savageau champions S systems: differential equations that capture kinetic interactions in a generalized, qualitative formalism. Thomas and Kauffman describe multistationarity in the context of Boolean networks.

25. Iglesias PA, Levchenko A: **Modeling the cell's guidance system**. *Sci STKE* 2002, **2002**:RE12.
26. Segel L: *Modeling Dynamic Phenomena in Molecular and Cellular Biology*. Cambridge: Cambridge University Press; 1984.
27. Goldbeter A: *Biochemical Oscillations and Cellular Rhythms*. Cambridge: Cambridge University Press; 1997.
28. Keener J, Sneyd J: *Mathematical Physiology*. Berlin: Springer; 1998.
29. Fall C, Marland E, Wagner J, Tyson J: *Computational Cell Biology*. Berlin: Springer; 2002.
30. Goldbeter A, Koshland DE: **An amplified sensitivity arising from covalent modification in biological systems**. *Proc Natl Acad Sci USA* 1981, **78**:6840-6844.
- 31. Levchenko A, Iglesias PA: **Models of eukaryotic gradient sensing: application to chemotaxis of amoebae and neutrophils**. *Biophys J* 2002, **82**:50-63.

This paper proposes a simple model for exact adaptation in sensory systems and applies the model to chemotactic motility of amoebae and neutrophils.

32. Knox BE, Devreotes PN, Goldbeter A, Segel LA: **A molecular mechanism for sensory adaptation based on ligand-induced receptor modification**. *Proc Natl Acad Sci USA* 1986, **83**:2345-2349.
33. Spiro PA, Parkinson JS, Othmer HG: **A model of excitation and adaptation in bacterial chemotaxis**. *Proc Natl Acad Sci USA* 1997, **94**:7263-7268.
34. Barkai N, Leibler S: **Robustness in simple biochemical networks**. *Nature* 1997, **387**:913-917.
35. Yi TM, Huang Y, Simon MI, Doyle J: **Robust perfect adaptation in bacterial chemotaxis through integral feedback control**. *Proc Natl Acad Sci USA* 2000, **97**:4649-4653.
36. Ferrell JE, Machleder EM: **The biochemical basis of an all-or-none cell fate switch in *Xenopus* oocytes**. *Science* 1998, **280**:895-898.
37. Novak B, Tyson JJ: **Numerical analysis of a comprehensive model of M-phase control in *Xenopus* oocyte extracts and intact embryos**. *J Cell Sci* 1993, **106**:1153-1168.
- 38. Kellershohn N, Laurent M: **Prion diseases: dynamics of the infection and properties of the bistable transition**. *Biophys J* 2001, **81**:2517-2529.

In describing simple mathematical models for the autocatalytic conversion of prion proteins into pathogenic forms, the authors of this paper use phase-plane and bifurcation diagrams to great advantage.

39. Sha W, Moore J, Chen K, Lassaletta A, Yi C, Tyson J, Sible J: **Hysteresis drives cell-cycle transitions in *Xenopus laevis* egg extracts**. *Proc Natl Acad Sci USA* 2002, in press.
- 40. Cross FR, Archambault V, Miller M, Klovstad M: **Testing a mathematical model of the yeast cell cycle**. *Mol Biol Cell* 2002, **13**:52-70.

This paper reports the first experimental demonstration of hysteresis in the eukaryotic cell cycle engine, confirming the predictions of Chen

et al. [9]. Cross *et al.* use elegant genetic manipulations of budding yeast cells to demonstrate the co-existence of stable G1 and S/G2/M steady states (low and high Cdk1–cyclin B activities, respectively).

41. Gardner TS, Cantor CR, Collins JJ: **Construction of a genetic toggle switch in *Escherichia coli***. *Nature* 2000, **403**:339-342.

•42. Becskei A, Seraphin B, Serrano L: **Positive feedback in eukaryotic gene networks: cell differentiation by graded to binary response conversion**. *EMBO J* 2001, **20**:2528-2535.

These authors engineered budding yeast cells to express proteins that constitute a mutual activatory feedback loop. They found two co-existing steady states, as expected, and that the system jumps spontaneously from the low to the high steady state because of random molecular noise in the cells.

43. Griffith JS: **Mathematics of cellular control processes. I. Negative feedback to one gene**. *J Theor Biol* 1968, **20**:202-228.

44. Goodwin BC: **An entrainment model for timed enzyme syntheses in bacteria**. *Nature* 1966, **209**:479-481.

45. Goldbeter A: **A minimal cascade model for the mitotic oscillator involving cyclin and cdc2 kinase**. *Proc Natl Acad Sci USA* 1991, **88**:9107-9111.

46. Kholodenko BN: **Negative feedback and ultrasensitivity can bring about oscillations in the mitogen-activated protein kinase cascades**. *Eur J Biochem* 2000, **267**:1583-1588.

47. Goldbeter A: **A model for circadian oscillations in the *Drosophila* period protein (PER)**. *Proc R Soc Lond Ser B* 1995, **261**:319-324.

48. Leloup JC, Goldbeter A: **Modeling the molecular regulatory mechanism of circadian rhythms in *Drosophila***. *Bioessays* 2000, **22**:84-93.

•49. Smolen P, Baxter DA, Byrne JH: **Modeling circadian oscillations with interlocking positive and negative feedback loops**. *J Neurosci* 2001, **21**:6644-6656.

These papers (see also Leloup and Goldbeter [2000] [49]) discuss in detail the molecular intricacies of circadian rhythmogenesis in fruit flies and bread molds. Leloup and Goldbeter study a long negative-feedback loop, as in Figure 2a. Smolen *et al.* consider models with both positive and negative feedback, and discrete time delays for transcription, translation and nuclear transport.

50. Elowitz MB, Leibler S: **A synthetic oscillatory network of transcriptional regulators**. *Nature* 2000, **403**:335-338.

51. Martiel J, Goldbeter A: **A model based on receptor desensitization for cyclic-AMP signaling in *Dictyostelium* cells**. *Biophys J* 1987, **52**:808-828.

52. Tyson JJ: **Modeling the cell division cycle: cdc2 and cyclin interactions**. *Proc Natl Acad Sci USA* 1991, **88**:7328-7332.

53. Guttman R, Lewis S, Rinzel J: **Control of repetitive firing in squid axon membrane as a model for a neuron oscillator**. *J Physiol* 1980, **305**:377-395.

54. Rupes I: **Checking cell size in yeast**. *Trends Genet* 2002, **18**:479-485.

55. Turing A: **The chemical basis of morphogenesis**. *Phil Trans R Soc Lond B* 1952, **237**:37-72.

56. Prigogine I, Lefever R: **Symmetry-breaking instabilities in dissipative systems**. *J Chem Phys* 1968, **48**:1695-1700.

57. Brenner S, Murray J, Wolpert L: *Theories of Biological Pattern Formation*. London: The Royal Society; 1981.

58. Tyson JJ, Murray JD: **Cyclic AMP waves during aggregation of *Dictyostelium amoebae***. *Development* 1989, **106**:421-426.

59. Bretschneider T, Siegert F, Weijer CJ: **Three-dimensional scroll waves of cAMP could direct cell movement and gene expression in *Dictyostelium* slugs**. *Proc Natl Acad Sci USA* 1995, **92**:4387-4391.

••60. Meinhardt H, de Boer PA: **Pattern formation in *Escherichia coli*: a model for the pole-to-pole oscillations of Min proteins and the localization of the division site**. *Proc Natl Acad Sci USA* 2001, **98**:14202-14207.

Using a model based on autocatalysis and substrate depletion, these authors describe FtsZ ring formation in *E. coli*, which determines the site of septum formation during cell division. Formation of the FtsZ ring in the midplane of the cell results from a spatial symmetry-breaking instability in the MinC/D/E reaction network.

••61. Hoffmann A, Levchenko A, Scott ML, Baltimore D: **The I κ B–NF- κ B signaling module: temporal control and selective gene activation**. *Science* 2002, **298**:1241-1245.

These authors present a satisfying combination of modeling and experimental studies of the NF- κ B signaling pathway, whose response is modulated by three isoforms of an inhibitor protein, I κ B α , - β and - ϵ . Expression of I κ B α is induced by NF- κ B, creating a negative-feedback loop that exhibits sustained oscillations when I κ B β and - ϵ are missing. An unexpected prediction of the model, that some NF- κ B-responsive genes might be efficiently activated by brief stimuli whereas others require longer exposure, was verified experimentally.

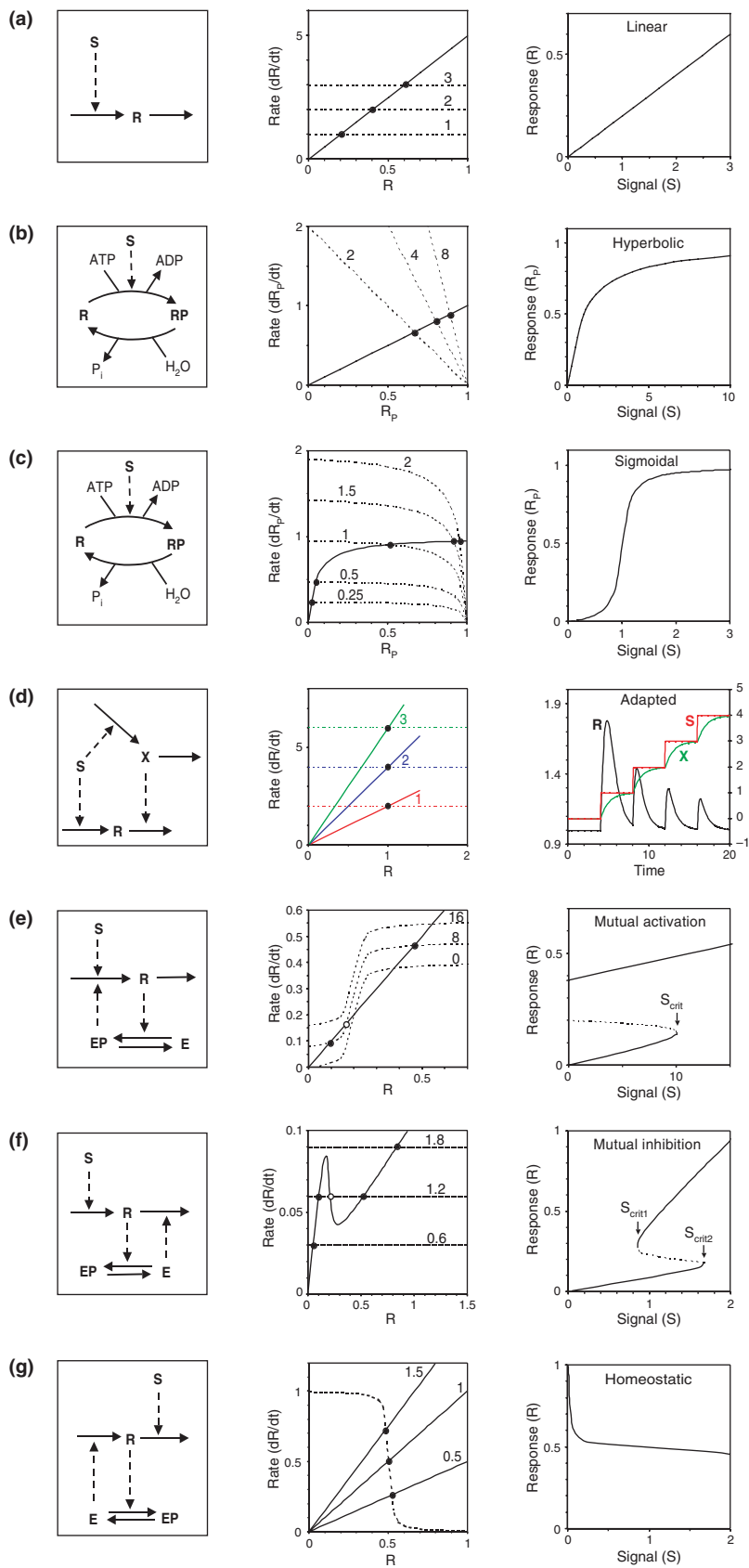
•62. Kholodenko BN, Kihatkin A, Bruggeman FJ, Sontag E, Westerhoff HV, Hoek JB: **Untangling the wires: a strategy to trace functional interactions in signaling and gene networks**. *Proc Nat Acad Sci USA* 2002, **99**:12841-12846.

See annotation Bruggeman *et al.* (2002) [68*].

•63. Bruggeman FJ, Westerhoff HV, Hoek JB, Kholodenko BN: **Modular response analysis of cellular regulatory networks**. *J Theor Biol* 2002, **218**:507-520.

In these papers (see also Kholodenko *et al.* [2002] [67*]), Kholodenko and colleagues describe new methods for deducing effective kinetic interactions within a reaction network, by analyzing its responses to many small perturbations.

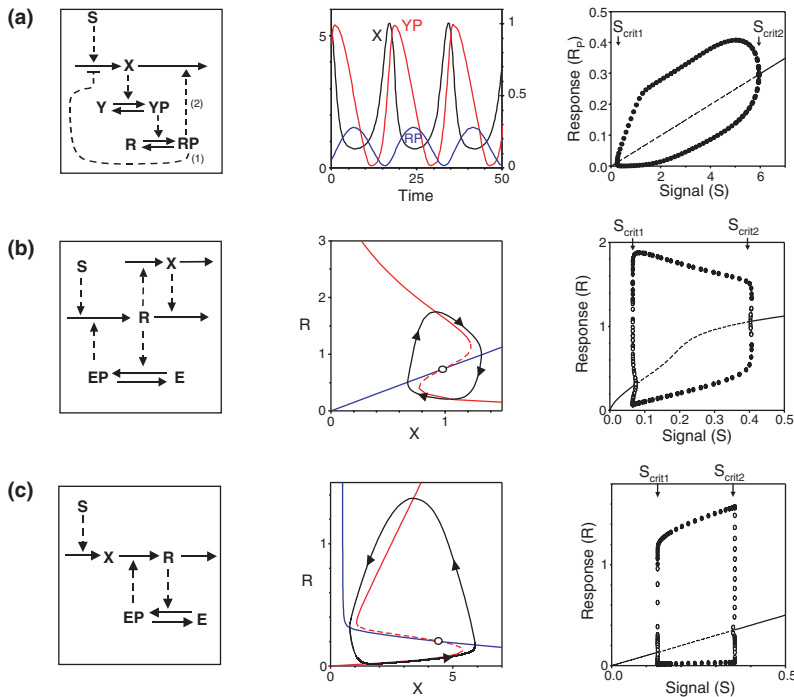
Figure 1



Signal-response elements. In this tableau, the rows correspond to **(a)** linear response, **(b)** hyperbolic response, **(c)** sigmoidal response, **(d)** perfect adaptation, **(e)** mutual activation, **(f)** mutual inhibition and **(g)** homeostasis. The columns present wiring diagrams (left), rate curves

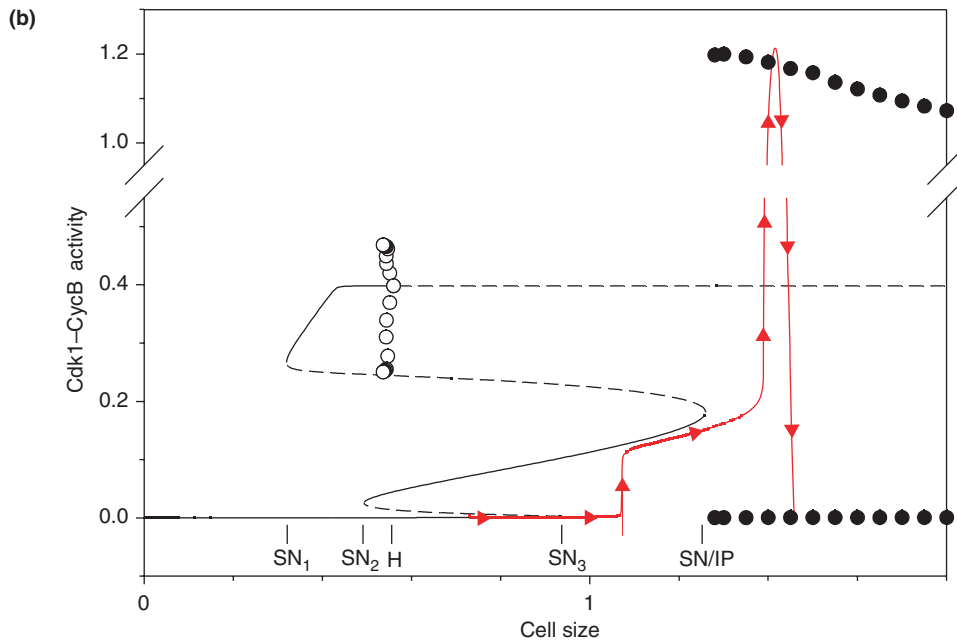
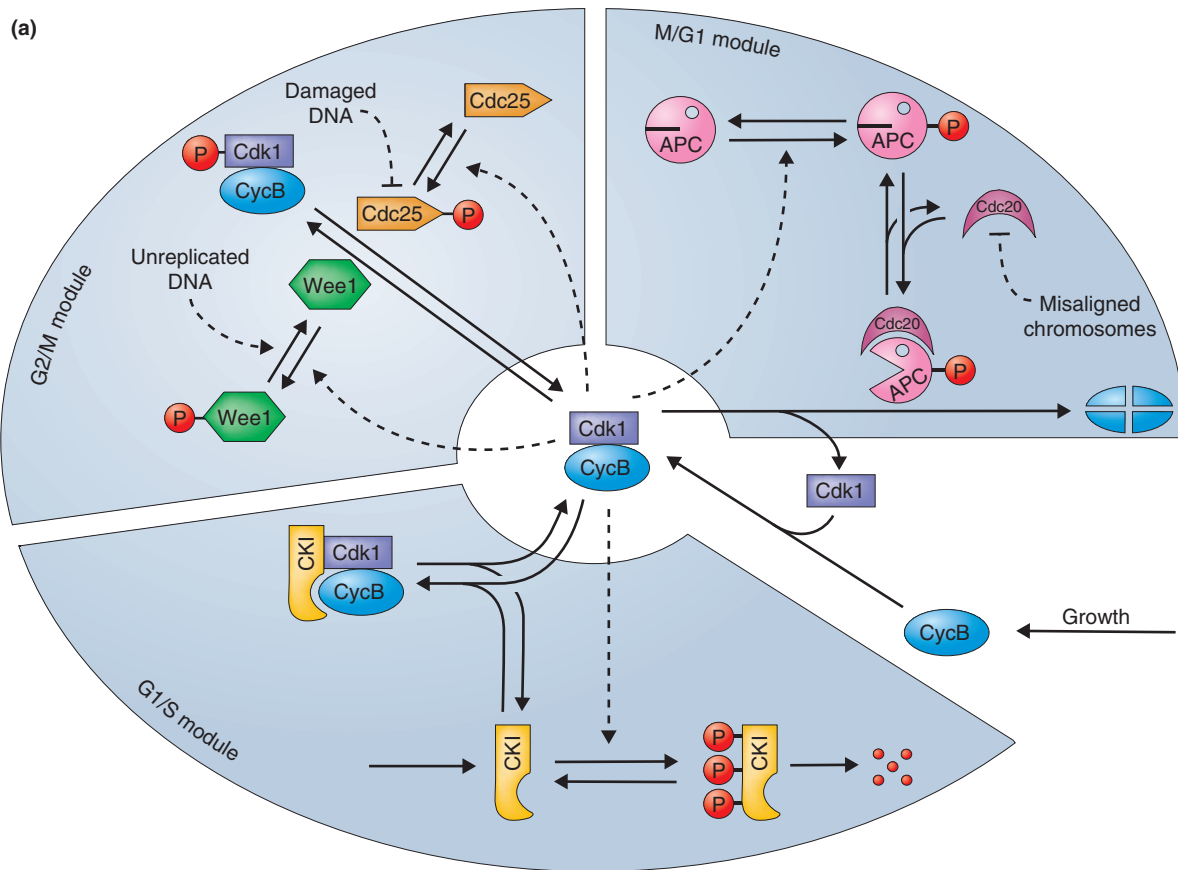
(center) and signal-response curves (right). From each wiring diagram, we derive a set of kinetic equations, which are displayed in the text (cases a, b and c) or in Box 1 (all other cases). The graphs in the center and right columns are derived from the kinetic equations, for the parameter values given in Box 1. In the center column (of most rows), the solid curve is the rate of removal of the response component (R or RP, depending on the context), and the dashed lines are the rates of production of the response component for various values of signal strength (the value of S is indicated next to each curve). The filled circles, where the rates of production and removal are identical, represent steady-state values of the response. In the right column, we plot the steady-state response as a function of signal strength. Row (d) is exceptional: both production and removal depend on signal strength, in such a fashion that the steady-state value of R is independent of S. Hence, the signal-response curve (not shown) is flat. Instead, we plot the transient response (R, black curve) to stepwise increases in signal strength (S, red curve), with concomitant changes in the indirect signaling pathway (X, green curve). Other symbols: P, inorganic phosphate; E, a protein involved with R in mutual activation or inhibition; EP, the phosphorylated form of E. In e) and (f), the open circle in the center column and the dashed curve in the right column represent unstable steady states. S_{crit} is the signal strength where stable and unstable steady states coalesce (a saddle-node bifurcation point).

Figure 2



Oscillatory networks. In this tableau, the rows correspond to **(a)** negative feedback, **(b)** activator-inhibitor and **(c)** substrate-depletion oscillators. The columns present wiring diagrams (left), (center) time courses (a) or phase planes (b,c), and signal-response curves (right). The kinetic equations corresponding to each wiring diagram are displayed in Box 1, along with the parameter values for which the other two columns are drawn. S, signal; R, response; E, X and Y, other components of the signaling network; EP, phosphorylated form of E; etc. (a) There are two ways to close the negative feedback loop: first, RP inhibits the synthesis of X; or second, RP activates the degradation of X. We choose case 2. Center column: oscillations of X (black, left ordinate), Y_p (red, right ordinate) and R_p (blue, right ordinate) for $S = 2$. Right column: the straight line is the steady-state response ($R_{P,ss}$) as a function of S; solid line indicates stable steady states, dashed line indicates unstable steady states. For a fixed value of S between S_{crit1} and S_{crit2} the unstable steady state is surrounded by a stable periodic solution. For example, the solution in the center column oscillates between $R_{P,max} = 0.28$ and $R_{P,min} = 0.1$. These two numbers are plotted as filled circles (at $S = 2$) in the signal-response curve to the right. S_{crit1} and S_{crit2} are so-called points of Hopf bifurcation, where small-amplitude periodic solutions are born as a steady state loses stability. Center column, (b,c): phase plane portraits for $S = 0.2$; red curve, (X,R) pairs that satisfy $dR/dt = 0$; blue curve, (X,R) pairs that satisfy $dX/dt = 0$; open circle, unstable steady state. Right column, (b,c): solid line, stable steady states; dashed line, unstable steady states; closed/open circles, maximum and minimum values of R during a stable/unstable oscillation. S_{crit1} and S_{crit2} are called subcritical Hopf bifurcation points.

Figure 3



Cell cycle regulation in eukaryotes. **(a)** Wiring diagram. Major events of the cell cycle are triggered by a cyclin-dependent kinase (Cdk1) in combination with cyclin B (CycB). The active dimer can be inactivated by combination with an inhibitor (CKI) or by phosphorylation of the kinase subunit by a kinase called Wee1. The inhibitory phosphate group is removed by a phosphatase (Cdc25). Cdk1-activity can also be destroyed by proteolysis of its cyclin partner, mediated by the anaphase-promoting complex (APC) in combination with Cdc20. **(b)** Signal-response curve. Solid black curve, stable steady states; dashed black curve, unstable steady states; filled circles, maximum and minimum of stable limit cycles; open circles, maximum and minimum of unstable limit cycles. The solid red curve indicates how the Cdk control system responds to a steady increase in cell size. A newborn cell (size = 0.73) starts at the left end of the red curve. As the cell grows, Cdk activity follows the red curve from left to right,

until the cell divides (at size = 1.46) and the process starts over again. SN_1 , SN_2 and SN_3 , saddle-node bifurcation points; H, Hopf bifurcation point (subcritical); SN/IP, saddle-node/infinite-period bifurcation point.

Box 1. Mathematical models of signal-response systems.

Figure 1d. Perfectly adapted

$$\frac{dR}{dt} = k_1 S - k_2 X \cdot R \quad R_{ss} = \frac{k_1 k_4}{k_2 k_3}$$
$$\frac{dX}{dt} = k_3 S - k_4 X \quad X_{ss} = \frac{k_3 S}{k_4}$$

Observe that R_{ss} is independent of S .

Figure 1e. Mutual activation

$$\frac{dR}{dt} = k_0 E_P(R) + k_1 S - k_2 R$$
$$E_P(R) = G(k_3 R, k_4, J_3, J_4)$$

Figure 1f. Mutual inhibition

$$\frac{dR}{dt} = k_0 + k_1 S - k_2 R - k_2' E(R) \cdot R$$
$$E(R) = G(k_3, k_4 R, J_3, J_4)$$

Figure 1g. Negative feedback: homeostasis

$$\frac{dR}{dt} = k_0 E(R) - k_2 S \cdot R$$
$$E(R) = G(k_3, k_4 R, J_3, J_4)$$

Figure 2a. Negative feedback oscillator

$$\frac{dX}{dt} = k_0 + k_1 S - k_2 X - k_2' R_P \cdot X$$
$$\frac{dY_P}{dt} = \frac{k_3 X (Y_T - Y_P)}{K_{m3} + Y_T - Y_P} - \frac{k_4 Y_P}{K_{m4} + Y_P}$$
$$\frac{dR_P}{dt} = \frac{k_5 Y_P (R_T - R_P)}{K_{m5} + R_T - R_P} - \frac{k_6 R_P}{K_{m6} + R_P}$$

Figure 2b. Activator inhibitor

$$\frac{dR}{dt} = k_0 E_P(R) + k_1 S - k_2 R - k_2' X \cdot R$$
$$\frac{dX}{dt} = k_5 R - k_6 X$$
$$E_P(R) = G(k_3 R, k_4, J_3, J_4)$$

Figure 2d. Substrate depletion

$$\frac{dX}{dt} = k_1 S - [k_0' + k_0 E_P(R)] \cdot X$$
$$\frac{dR}{dt} = [k_0' + k_0 E_P(R)] \cdot X - k_2 R$$
$$E_P(R) = G(k_3 R, k_4, J_3, J_4)$$

Parameter sets

1A $k_0 = 0.01, k_1 = 1, k_2 = 5$

1B $k_1 = k_2 = 1, R_T = 1$

1C $k_1 = k_2 = 1, R_T = 1, K_{m1} = K_{m2} = 0.05$

1D $k_1 = k_2 = 2, k_3 = k_4 = 1$

1E $k_0 = 0.4, k_1 = 0.01, k_2 = 1, k_3 = 1, k_4 = 0.2, J_3 = J_4 = 0.05$

1F $k_0 = 0, k_1 = 0.05, k_2 = 0.1, k_2' = 0.5, k_3 = 1, k_4 = 0.2, J_3 = J_4 = 0.05$

1G $k_0 = 1, k_2 = 1, k_3 = 0.5, k_4 = 1, J_3 = J_4 = 0.01$

2A $k_0 = 0, k_1 = 1, k_2' = 10, k_2 = 0.01, k_3 = 0.1, k_4 = 0.2, k_5 = 0.1, k_6 = 0.05, Y_T = 1, R_T = 1, K_{m3} = K_{m4} = K_{m5} = K_{m6} = 0.01$

2B $k_0 = 4, k_1 = 1, k_2 = 1, k_2' = 1, k_3 = 1, k_4 = 1, k_5 = 0.1, k_6 = 0.075, J_3 = J_4 = 0.3$

2C $k_0' = 0.01, k_0 = 0.4, k_1 = 1, k_2 = 1, k_3 = 1, k_4 = 0.3, J_3 = J_4 = 0.05$
